



Microcontainers as an oral delivery system for spray dried cubosomes containing ovalbumin

Nielsen, Line Hagner; Rades, Thomas; Boyd, Ben J; Boisen, Anja

Published in:
European Journal of Pharmaceutics and Biopharmaceutics

DOI:
[10.1016/j.ejpb.2016.12.008](https://doi.org/10.1016/j.ejpb.2016.12.008)

Publication date:
2017

Document version
Peer reviewed version

Document license:
[CC BY-NC-ND](#)

Citation for published version (APA):
Nielsen, L. H., Rades, T., Boyd, B. J., & Boisen, A. (2017). Microcontainers as an oral delivery system for spray dried cubosomes containing ovalbumin. *European Journal of Pharmaceutics and Biopharmaceutics*, 118, 13-20. <https://doi.org/10.1016/j.ejpb.2016.12.008>

Microcontainers as an oral delivery system for spray dried cubosomes containing ovalbumin

Line Hagner Nielsen^{1,A}, Thomas Rades², Ben Boyd³, Anja Boisen¹

¹Department of Micro and Nanotechnology, Technical University of Denmark, Kgs. Lyngby, Denmark

²Department of Pharmacy, Faculty of Health and Medical Sciences, University of Copenhagen, Copenhagen, Denmark

³Monash Institute of Pharmaceutical Sciences, Monash University, Melbourne, Australia

^ACorresponding author: Technical University of Denmark, DTU Nanotech, Building 345C, Kongens Lyngby, Denmark. Tel: +4545256843 Fax: + 4545887762 E-mail address: lihan@nanotech.dtu.dk (L. Hagner Nielsen).

14 **Abstract**

15 The purpose of this study was to prepare cubosomes encapsulating the model antigen ovalbumin (OVA) via
16 spray drying, and to characterise such cubosomes with a view for their potential application in oral vaccine
17 delivery. Furthermore the cubosome formulation was loaded into polymeric microcontainers intended as
18 an oral drug delivery system. The cubosomes consisted of commercial glyceryl monooleate, Dimodan®,
19 containing OVA and were surrounded with a dextran shell prepared by spray drying. Cryo-TEM was used to
20 confirm that cubosomes were formed after hydration of the spray dried precursor powder. The precursor
21 powder had a mean particle size of $1.3 \pm 0.1 \mu\text{m}$, whereas the mean diameter of the dispersed cubosomes
22 was $282 \pm 7 \text{ nm}$ (PDI: 0.18) measured by dynamic light scattering. $8.5 \pm 0.3 \%$ (w/w) of OVA was present in the
23 cubosome powder and OVA was found released slowly over the first 70 h, followed by a more rapid
24 release. Total release of $47.9 \pm 2.8 \%$ of loaded OVA occurred over 96 h in a buffer at pH 6.8. When the
25 powder was filled into microcontainers, and the opening covered with the pH sensitive polymer Eudragit
26 S100, the pH sensitive 'lid' was intact at gastric pH, but release of OVA from the cubosomes and
27 microcontainers occurred at pH 6.8, releasing $44.1 \pm 5.6 \%$ of the OVA in 96 h. Small-angle X-ray scattering
28 (SAXS) revealed that the 'dry' particles possessed an internal ordered lipid structure (lamellar and inverse
29 micellar phase) by virtue of a small amount of residual water, and after hydration in buffer at pH 6.8, the
30 particles formed the hexagonal inverse cubic phases, thereby indicating that cubosomes were formed
31 when released from microcontainers.

Introduction

Vaccination is often regarded as the most significant contribution to public health and disease prevention and moreover, it is a very cost-effective medical intervention [1,2]. Vaccination has reduced the morbidity and mortality resulting from diseases such as tuberculosis and smallpox and has thereby saved millions of lives. In spite of this, many infectious diseases remain endemic in large parts of the world, and therefore vaccination is an area in continuous development [1,2].

Most vaccines are administered by injection and there are only a few oral vaccines on the market such as rotavirus vaccine (as solution or suspension) and a capsule with vaccine formulation against typhoid fever [3]. Although, the oral route can be beneficial for vaccine administration [4,5]. Some of the advantages of oral vaccines are the ease of administration and an increased safety compared to injections. In addition, there is also a great potential for mass vaccination without the requirements of trained personnel [4,6]. Furthermore, oral vaccines have the ability to induce both mucosal and systemic immune responses [6,7], as shown in the 1990s with several HIV vaccines [8], and they are therefore considered ideal for combating infectious diseases. Although, oral vaccines have several attractive features, there are some major challenges.

The target of vaccine formulations in the gastro-intestinal (GI) tract is the M-cells in the intestine [9]. The antigen might be damaged, when passing through the harsh environment of the GI tract, which in turn will lead to the need for large doses. In addition, there is a poor transport of the antigen across the intestinal epithelium [4].

Traditional vaccines are mainly composed of heat-inactivated bacteria or viruses resulting in high immunogenicity. The risk with these types of vaccines is that they, in the body, can change to the active state and thereby infect the patients with the bacteria or virus and thus, leading to unwanted side effects [1,10]. Consequently, new generation vaccines are developed with subunit antigens. These subunit antigens are highly purified components of pathogens and thereby chemically well-defined. Hence, there is a much higher safety than for traditional antigens, but as the subunit antigens lack most of the features of the original pathogen they tend to be poorly immunogenic [1,10]. Therefore, to succeed with oral vaccine delivery, delivery systems need to be developed, in which the antigen can be encapsulated into particles [11,12]. These particles will assure presentation of the antigen to the antigen-presenting cells, but can also stabilise and release the antigen over an extended period of time [10]. Some particles will provide an adjuvant effect in themselves, but potent adjuvants can in addition also be added to the particulates for inducing an effective immunity [13].

There are many possibilities for vaccine delivery systems, and some of the most common ones are: polymeric micro- and nanoparticles, immunostimulatory complexes and liposomes [14,15]. Cubosomes have also shown to be an efficient delivery system for vaccines [11]. Cubosomes contain a highly twisted, continuous lipid bilayer with two congruent, non-intersecting water channels, giving the particles both hydrophobic and hydrophilic domains [11]. This offers great flexibility with respect to the types of compounds, that can be incorporated into the particles [16,17]. Rizwan et al. found that significantly higher amounts of antigen can be encapsulated in cubosomes compared to liposomes due to the larger surface area of cubosomes, and moreover in cubosomes, the antigen was also retained more efficiently compared to liposomes [11].

Traditionally, cubosomes are produced by mixing monoolein or phytantriol and water and thereby creating a high-energy dispersion followed by colloidal stabilisation using polymeric stabilisers [11,18,19]. However, it can be desirable to have the vaccine particles in a powder form (here termed “precursors”), and precursors of cubosomes have earlier been produced by either freeze drying [20] or spray drying [21–23]. In the spray drying process, dry powder precursors have the active ingredient incorporated, and upon hydration colloiddally stable cubosomes are spontaneously formed. The powder form of the vaccine formulation can be advantageous in terms of stability of the antigen. Also, there is no need for a cold-chain storage which is needed for traditional vaccines [4].

After oral administration of the vaccine formulations, the antigen needs to be protected in the stomach and during transportation to the small intestine. In the small intestine, the vaccine particles should be delivered to the microfold (M) cells of the peyer’s patches as they will present the antigen to the underlying immune cells and thereby obtain an immune response [24]. The particles, carrying the antigen (and adjuvant), can give some protection of the antigen through the GI environment, but often the particles will also degrade on the way to the intestine, and therefore more advanced drug delivery systems can be necessary. An example of these advanced drug delivery systems is microcontainers. Microcontainers are polymeric, cylindrical devices in the micrometre size range (Fig. 1) [25–27]. They have the potential for targeted and/or sustained delivery in the GI tract [28]. Some of the advantages of the microcontainers are that size and shape can be controlled very precisely. Furthermore, the devices allow for unidirectional release, as only one side of the microcontainer is open, compared to more conventional microparticles where release can occur from the whole surface area. This has shown to increase the drug concentration at the microdevice-cell interface and thereby, allowing for increased permeation of the drug *in vitro* leading to enlarged oral bioavailability of the drug [27,29,30]. In addition, the antigen can be protected inside the cavity of the microcontainer from the harsh environment of the stomach until release is desirable [31,32]. The microcontainers have previously shown to interact with the intestinal mucus resulting in prolonged drug absorption [27]. It is reported in the literature that one way to improve oral vaccine delivery is to extend the intestinal residence time [13], hence, the microcontainers can be a promising platform for this purpose. In this paper, SU-8 (an epoxy photoresist) was used as a model polymer for fabrication of the microcontainers [25,26,31], but microcontainers have also been fabricated using biopolymers such as poly-L-lactic acid (PLLA) [33,34].

The aim of this study was, as a proof-of-concept, to prepare and characterise cubosomes loaded with ovalbumin (OVA) in a spray dried powder form for future application in oral vaccine delivery. The precursor powder was filled into microcontainers for protection and release control, and the *in vitro* release was studied together with small-angle X-ray scattering (SAXS) to confirm whether cubosomes were released from the microcontainers as internally structured particles.

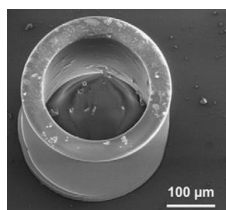


Fig. 1: SEM image of an SU-8 microcontainer with an inner diameter of 223 μm [26].

114
115
116
117
118
119
120
121
122
123
124
125
126
127
128
129
130
131
132
133
134
135
136
137
138
139
140
141
142
143
144
145
146
147
148
149
150
151
152
153
154
155
156

Materials and methods

Materials

OVA was purchased from TCI Europe (Zwijndrecht, Belgium). Dimodan® D90 was kindly donated by Danisco (Grindsted, Denmark). Dextran (from *Leuconostoc Mesenteroides*) and potassium dihydrogen phosphate were acquired from Sigma-Aldrich (St. Louis, MO, USA). Pierce BCA Protein Assay kit was purchased from Thermo Fisher Scientific (Rockford, IL, USA). Deionised water was obtained from an SG Ultra Clear water system (SG Water USA, LLC, Nashua, NH, USA) and was freshly produced in all cases. All other chemicals used were of analytical grade.

Spray drying of precursors for cubosomes containing OVA

Cubosomes were prepared using a commercial source of glyceryl monooleate (GMO), Dimodan® MO 90/D. The cubosomes were loaded with OVA as a model antigen, and the particles were surrounded by a dextran shell. The particles were prepared by first dissolving GMO in ethanol (1.78 w/v %), and then mixing with a solution of OVA in MilliQ water (0.075 final w/w % of OVA). After 1 h of mixing, dextran dissolved in MilliQ water (1.77 w/v %) was added to the GMO/OVA solution (0.72 w/w % of GMO + OVA), and the final solution was spray dried using a B 290 Büchi mini spray dryer (Büchi Labortechnik AG, Flawil, Switzerland). Free OVA was not removed prior to the spray drying process.

For the spray drying of the precursors, a 0.7-mm nozzle was used and air was utilised as the drying medium. Spray drying was performed at an inlet temperature of 200 °C resulting in an outlet temperature of approximately 85 °C. The drying flow rate was set to 32 m³/h and an aspirator capacity of 80 % with a feed rate of 4 mL/min was used. Particles without OVA were also produced as blank particles and used as reference.

Cryo-TEM of cubosomes

The precursors for the cubosomes with OVA were dispersed in MilliQ water at a concentration of 1 mg/mL. The samples for the Cryo-TEM studies were prepared in a controlled environment vitrification system (CEVS). A small amount of the sample (5 µL) was put on a carbon film supported by a copper grid and blotted with filter paper to obtain a thin liquid film on the grid. The grid was quenched in liquid ethane at –180 °C and transferred to liquid nitrogen (–196 °C). The samples were then examined using a Tecnai G2 F30 Transmission Electron Microscope (FEI, Eindhoven, The Netherlands) operating at a voltage of 300 kV and a working temperature of –180 °C. Images were recorded using Gatan UltraScan 1000 (2k × 2k) CCD camera (Gatan, California, USA).

Size of particles

The size of the dry particles with the dextran shell was measured using aerosizer particle size analyser (Model 3321, TSI Incorporated, MN, USA) by setting the pump to 1.37 bar and with a capillary flow of 8 L/min. A small amount of powder was distributed on the plate and the particle size was measured in six replicates.

For the particles dispersed in water, the particle size distribution (Z-average), polydispersity (PDI) and zeta potential were determined using dynamic light scattering (Malvern Zetasizer, NanoZs ZEN 3600, Malvern, UK). Measurements were performed at 37°C, and the results presented are the mean of three successive

157 measurements of 100 s of at least three independent samples. Samples were diluted with water to adjust
158 the signal level.

159

160 OVA present in the cubosomes

161 Precursor powder (10 mg) was added to a solution of 20 mM phosphate buffer, pH 6.8 containing 5 %
162 Triton X-100. After vortex mixing, the cubosomes were dissolved and a sample of 200 μ L was taken out. A
163 BCA Protein Assay kit was used to determine how much OVA was present in the cubosome powder by
164 following the procedures for the standards and samples recommended by the manufacturer. The same
165 process was performed with the blank cubosomes to check for any cross activity of the formulation. The
166 absorbance was measured at 562 nm on a plate reader, and the obtained absorbance values were analysed
167 against the standard curves prepared on the same day as the samples. OVA entrapment was then
168 determined by calculating the difference between the total OVA added before the spray drying process and
169 the free fraction of OVA in the solution. The experiments were performed in triplicates.

170

171 Fabrication of SU-8 microcontainers

172 Production of the microcontainers involved two steps of photolithography with the negative epoxy-based
173 photoresist, SU-8 [26,32]. The microcontainers were structured on a fluorocarbon coating deposited on top
174 of the supporting silicon wafer by plasma polymerisation. This enabled dry removal of the fabricated SU-8
175 devices from the support substrate in order to obtain individual microcontainers if needed [27,35]. The
176 fabricated microcontainers had an inner diameter of 223 ± 3 μ m and a height of 270 ± 3 μ m (mean \pm SD, n=6).
177 Silicon wafers supporting the microcontainers were finally cut into squares of 12.8×12.8 mm² using an
178 Automatic Dicing Saw from DISCO (Kirchheim b. München, Germany). Each chip contained arrays of 25×25
179 containers with a pitch of 450 μ m.

180

181 Filling of microcontainers with powder precursors

182 Powder precursors were manually distributed on the microcontainer chip. The excess drug in between the
183 microcontainers was then removed with pressurised air, resulting in powder-filled microcontainers [27].
184 The chip with microcontainers was weighed before and after filling to determine the amount of drug filled
185 into the microcontainers.

186

187 Spray coating of the filled microcontainers with Eudragit S100

188 A spray coating system (ExactaCoat, Sono Tek, USA) equipped with an ultrasonic nozzle actuated at 120 kHz
189 [36] was used to deposit Eudragit S100 (dissolved to a 2 % (w/w) solution in isopropyl alcohol) on the cavity
190 of the drug-filled microcontainers in a set-up similar to previously described [33]. The generator power was
191 set to 1.5 W, and the polymer solution was pumped through the nozzle at a flow rate of 100 μ L/min.
192 Nitrogen gas at a pressure of 10 mbar was used to direct the beam of droplets onto the microcontainers,
193 and the distance between nozzle and substrate was 40 mm with the beam diameter on the substrate being
194 approximately 4 mm. The lateral movements of the nozzle were controlled by an x-y stage and the nozzle
195 path was defined in the equipment software. The nozzle was moved line-by-line at a speed of 25 mm/s, and
196 the coating was repeated 60 times to obtain a coating thickness in the μ m range.

197

198 Release of OVA from the cubosomes

199 *In vitro* release of OVA from the cubosomes unconfined (bulk powder) and confined in microcontainers
200 coated with Eudragit S100 was investigated on a μ DISS profiler (pION INC, Woburn, MA). In both release
201 studies, each channel was calibrated with its own OVA standard curve prior to the experiments. For the
202 calibration curves, aliquots of OVA in water stock solution were repeatedly added to 10 mL of either a HCl
203 solution or a phosphate buffer in order to achieve a range of defined standard concentrations, and the UV
204 spectrum of each standard was recorded. The release experiments were performed at $37\pm0.5^\circ\text{C}$ using a
205 stirring rate of 200 ± 5 rpm using 20 mm path length *in situ* UV probes on a μ DISS profiler. The absorbance
206 data was evaluated using 280 nm on the standard curve and utilising the 2nd derivative function in the Au
207 Pro software affiliated with the μ DISS profiler.

208

209 The release of OVA from the precursor powder was studied in 20 mM phosphate buffer, pH 6.8 for 96 h.
210 The *in situ* UV probes were situated in each sample vial containing 10 mg of powder and 10 mL of
211 phosphate buffer was added. The probes scanned and detected the absorbance of released OVA.

212 The release studies from the microcontainers were performed in a set-up similar to one previously
213 described [25,27,33]. The chips with microcontainers were attached to cylindrical magnetic stirring bars
214 (using carbon pads) and placed in the bottom of sample vials. The chips were covered with 10 mL of 0.1 M
215 HCl pH 1.6 for 2 h and subsequently, the medium was changed to 10 mL of 20 mM phosphate buffer, pH
216 6.8 for 96 h, and the *in situ* UV probes detected the absorbance.

217 Both sets of experiments were performed in 3 replicates.

218

219 Scanning electron microscopy of the microcontainers

220 SEM was utilised to examine the microcontainers after filling, after spray coating of the lid of Eudragit S-
221 100, and after release in phosphate buffer at pH 6.8. The examinations were carried out using a Phenom
222 Pro scanning electron microscope (Phenom World, Eindhoven, the Netherlands). Prior to the investigations,
223 the microcontainer chip was mounted onto metal stubs, and imaging was performed at an operation
224 voltage of 10kV with a 600x magnification.

225

226 SAXS determination of the structure of cubosomes loaded into microcontainers

227 The SAXS/WAXS beamline at the Australian Synchrotron, Clayton, Australia [37] was used to determine the
228 internal structure of the spray dried particles, when the cubosomes were confined in microcontainers and
229 released from the devices. The X-ray beam had an energy of 11 keV, and the 2D SAXS patterns were
230 collected using a Pilatus 1M camera (active area $169 \times 179 \text{ mm}^2$ with a pixel size of $172 \times 172 \mu\text{m}$), which
231 was located 900 mm from the sample position. The total q range for the instrument configuration outlined
232 above was $0.02 < q < 1.06 \text{ \AA}^{-1}$, and 2D SAXS patterns were collected for 1 sec. The in-house designed
233 computer software 'ScatterBrain' was used to acquire and reduce these 2D patterns to 1D intensity versus
234 q profiles. The powder-filled microcontainers were separated from the base using a scalpel, and filled into a
235 1.5 mL capillary and SAXS patterns were acquired in dry state followed by addition of 50 μL of MilliQ water,
236 where after patterns were acquired for a time period of 80 min. The set-up with empty microcontainers as
237 an example can be seen in Fig. 2A, with an image of the microcontainers in a capillary in the X-ray beam
238 shown in Fig. 2B.

239

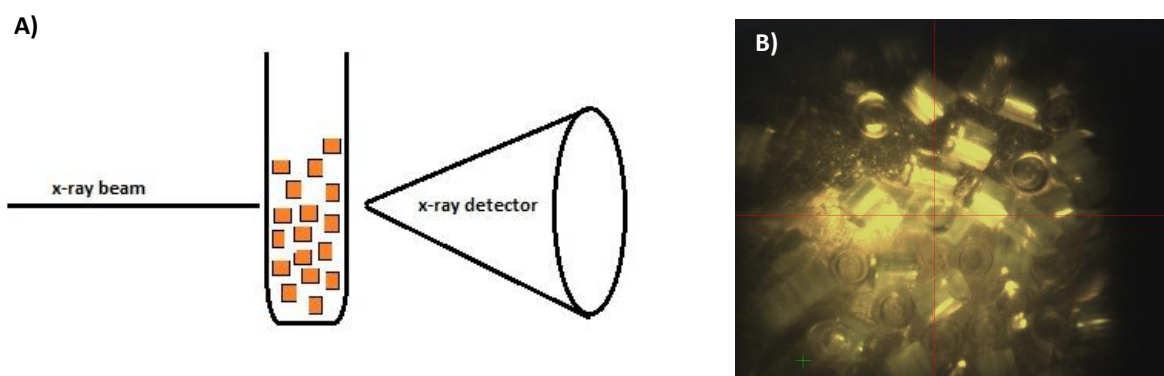


Fig. 2: A) Schematic of the SU-8 microcontainers filled into a capillary to be used in the SAXS/WAXS synchrotron. B) Micrograph showing the set-up with the microcontainers in the x-ray beam.

Statistics

The data are expressed as mean \pm standard deviation (SD). Where appropriate, statistical analysis was carried out using Student t-tests using GraphPad Prism version 7.00 (GraphPad Software Inc., CA, USA). P-values below 5 % ($p < 0.05$) were considered statistically significant.

Results and discussion

For the production of the powder precursors of cubosomes, spray drying was chosen as this is a simple technique converting a solution to powder in a one-step process [38]. GMO has for many years been one of the lipids of choice for producing cubosomes, as it is non-toxic, biocompatible and biodegradable [39], and therefore it was decided to produce GMO particles in this study. The spray drying technique is convenient for producing the powder precursors, but GMO can be challenging to spray dry as it immediately forms the cubic phase upon hydration. Spicer et al. studied the effect of applying ethanol as a hydrotrope and this resulted in the formation of a low-viscous emulsion that was easily spray dried [21]. For this reason, in this study, GMO was first dissolved in ethanol and then added to the aqueous dextran solution. It has been reported that GMO itself produces sticky agglomerates after spray drying, and to obtain a more flowable powder an aqueous starch or a dextran solution can be added prior to spray drying resulting in the GMO being encapsulated in a dry starch or dextran shell [21–23]. In this work, it was chosen to add dextran as the anti-cohesion agent, and the produced powder was flowable and easy to hydrate. After production of the GMO powder precursors, the powder was hydrated and cryo-TEM was performed to identify whether cubosomes were obtained. It can be observed in Fig. 3 that cubic structures were found after hydration of the powder.

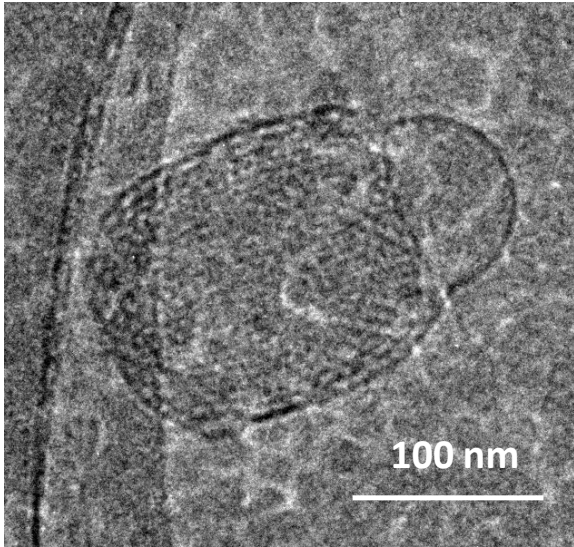


Fig. 3: Cryo-TEM image of a representative hydrated particle with a distinct cubic liquid crystalline structure. The resolution in cryo-TEM images is limited by the presence of dissolved dextran.

In vitro characterisation of the particulates

The size, shape and surface charge of a particulate vaccine carrier will influence its performance as a vaccine [40]. The dry powder with OVA and the dextran shell had a size of $1.3 \pm 0.1 \mu\text{m}$, whereas the dry blank particles without OVA had a size of $1.6 \pm 0.1 \mu\text{m}$. After hydration, self-assembled, close to neutrally charged nanoparticles were formed, with mean size of $146.1 \pm 1.3 \text{ nm}$ and $281.7 \pm 7.4 \text{ nm}$ for the blank and OVA-loaded particles, respectively (Table 1). There was a significant size difference between the blank and OVA-loaded particles ($p\text{-value} < 0.0001$), and the PDI for both formulations was low, indicating homogeneous formulations. The particles were much smaller than those reported by Spicer et al., where the dry particles had a diameter of $24 \mu\text{m}$, and in the hydrated form the cubosomes were in average $0.6 \mu\text{m}$ with a size distribution from 0.1 to $5 \mu\text{m}$ [22]. In general, it is reported that the particle size should be between 20 nm to $10 \mu\text{m}$ to be well recognised by the immune system [11], but more specifically for oral vaccine formulations, a size between $200\text{-}500 \text{ nm}$ can be advantageous for uptake into the antigen-presenting cells after oral administration [40,41]. In relation to this, it can be observed that the size of the cubosomes with OVA is in this size range, and the cubosomes should therefore be able to be taken up by the antigen-presenting cells.

Table 1: Size measurements of the hydrated cubosomes with and without OVA dispersed in MilliQ water. The measurements were performed using dynamic light scattering in triplicates, and data are represented as mean \pm SD

	Z-average (nm)	PDI	Zeta potential (mV)
Blank particles	146.1 ± 1.3	0.15 ± 0.02	-0.43 ± 0.077
Particles with OVA	281.7 ± 7.4	0.18 ± 0.11	-0.18 ± 0.042

Presence and release of OVA in and from the particles

Before the release measurements, it was initially determined that $8.5 \pm 0.3 \%$ (w/w) OVA was present in the cubosome powder. It is also well-known that cubosomes often provide a sustained release of a drug [39], and this is also observed in this study, where release studies in buffer at pH 6.8 showed that during the first

70 h, OVA was slowly released, followed by a more rapid release from 70-80 h. A total release of $47.9 \pm 2.8\%$ was observed in relation to the total loading of OVA in the cubosomes over a 96 h period (Fig. 4). It can be seen that there is a significant burst release of OVA from the cubosomes (insert in Fig. 4) of $18.2 \pm 1.6\%$ in the first 10 min. This is probably caused by the release of OVA from the powder just when the powder precursors are dispersed in the aqueous solution, and thereafter the OVA entrapped in the channels of the cubosomes is released. In the literature, it is reported that OVA was released during 168 h from cubosomes resulting in a complete release [18]. A study preparing precursors of cubosomes by spray drying, but encapsulating the highly lipophilic drug, efavirenz, also is reporting on a burst release of the drug of up to 16 %, with a total release in 12 h of up to 56 %, again indicating that when dispersing powder precursors in aqueous solution a burst release is occurring [23]. A sustained release of OVA is also observed in this study and this could be beneficial when developing vaccine formulations [42].

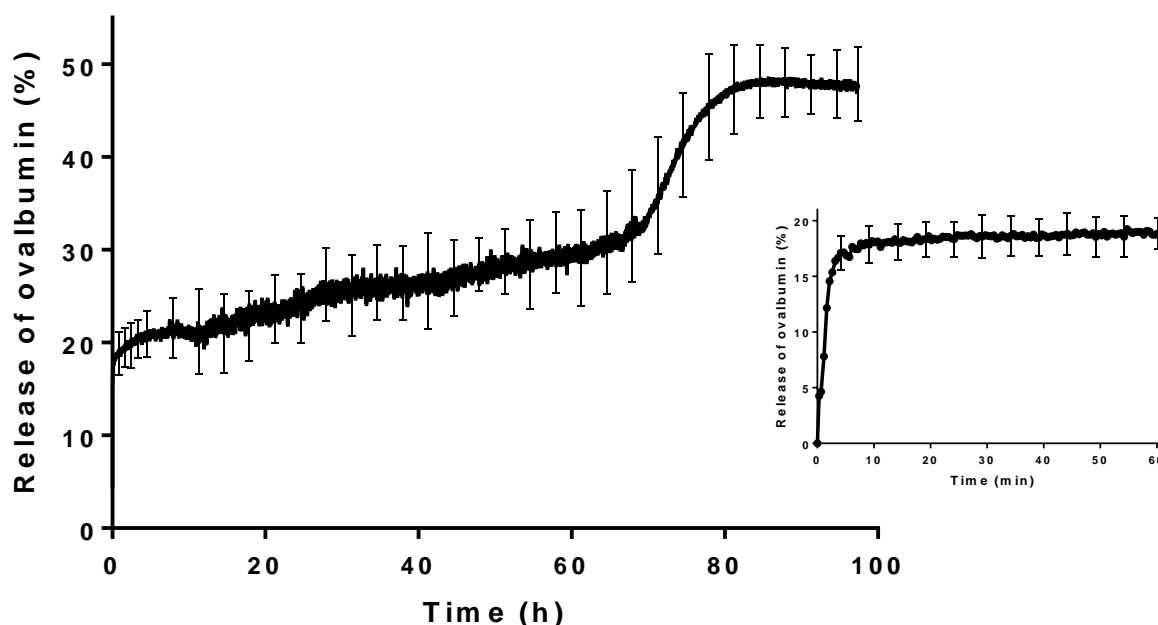


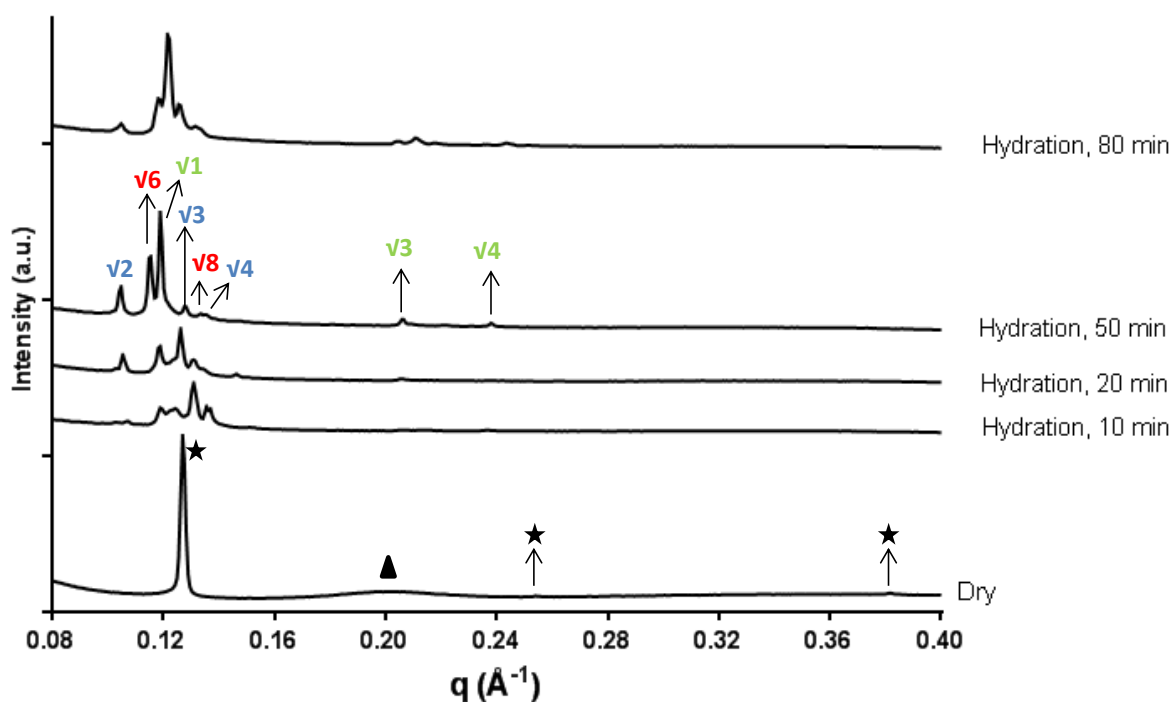
Fig. 4: Release of OVA from the cubosomes in 20 mM phosphate buffer pH 6.8, expressed as % of the total content of OVA. The insert is showing the release over the first 60 min. The release study was performed in triplicates, and the data represent mean \pm SD.

Internal structure of particles formed upon hydration from microcontainers

SAXS/WAXS can be used to detect phase transformations in self-assembled lipid systems, and this was utilised to identify whether particles released from the microcontainers contained internal nanostructures consistent with cubosomes. Fig. 5 shows the plot of intensity versus the scattering vector q obtained from the release of GMO particles in dry form and when the microcontainers containing the particles were dispersed in water for a period of 80 min. For the dry particles, it can be observed that there are three equally spaced peaks in the diffractogram (Fig. 5), indicating that the dry particles are in a lamellar phase with the lattice parameter of 49.5 \AA (Table 2). There is also an inverse micellar phase present, indicated by the broad peak at $q \sim 0,2 \text{ \AA}^{-1}$ in the diffractogram) with a D-spacing of 31.1 \AA . This can be explained by the

320 presence of residual moisture in the spray dried powder. According to the phase diagram of GMO in water,
 321 the inverse micellar phase and lamellar phase coexist at approximately 5 % water [43,44], consistent with
 322 Spicer et al. reporting approximately 5 % (w/w) of moisture content in their spray dried cubosome powders
 323 [22].

324
 325 After hydration (here exemplified by the diffractogram at 50 min), the liquid crystalline nanostructured
 326 particles showed a mix of phases, with peak indexing indicating coexisting inverse hexagonal (H_2) phase
 327 (peaks at $v1 : v3 : v4$), . Pn3m cubic phase (peaks at $v2 : v3 : v4$), and la3d cubic phase (peaks at $v6 : v8$).
 328 These three phases appear in the GMO + water phase diagram [44], and the calculated lattice parameters
 329 are listed in Table 2. The presence of H_2 and Pn3m cubic phases for commercial GMO samples in water
 330 might be expected at full hydration, however the la3d cubic phase is only expected at less than full
 331 hydration o the lipid. Therefore it is proposed that the particles were not completely hydrated after 50 min,
 332 which is also supported by the fact that after 80 min the la3d phase appears even less prominent.
 333



334
 335 Fig. 5: 2D SAXS patterns were collected from cubosomes confined in microcontainers and followed while
 336 the cubosomes were released from the microcontainers in MilliQ water. The cubosome filled
 337 microcontainers were enclosed in a glass capillary during hydration for up to 80 min. After 50 min of
 338 hydration the particles show a mix of phases with inverse hexagonal (H_2) phase (peaks at $v1 : v3 : v4$),
 339 Pn3m cubic phase (peaks at $v2 : v3 : v4$), and la3d cubic phase (peaks at $v6 : v8$).
 340
 341
 342

343 Table 2: Phase structure and lattice parameters obtained from SAXS measurements of dry particles and
 344 particles released from microcontainers after hydration, here with an example after 50 min of hydration.

	Lattice parameters (Å)	
	Dry particles	Hydration for 50 min
Lamellar phase, L_{α}	49.5	
Inverse micellar phase, L_2	31.1	
Inverse hexagonal phase, H_2		61.0
Inverse bicontinuous cubic phase, $Pn3m$		84.6
Inverse bicontinuous cubic phase, $Ia3d$		132.7

Loading of precursors into the microcontainers and coating of the pH sensitive lid

After successfully loading the cubosomes into the microcontainers (Fig. 6A), the cavity of the microcontainers was coated with Eudragit S100 (Fig. 6B) as this polymer will dissolve at a pH value of approximately 7 corresponding to the pH found in the small intestine around the M cells [9].

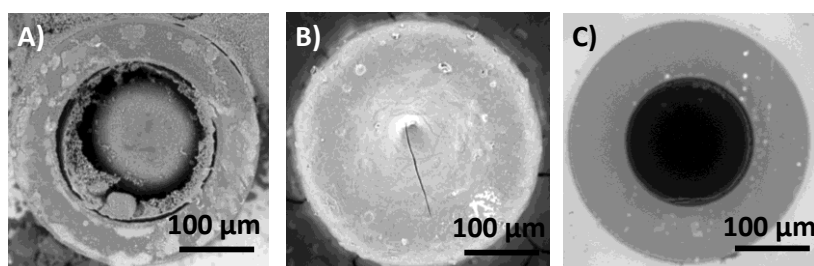


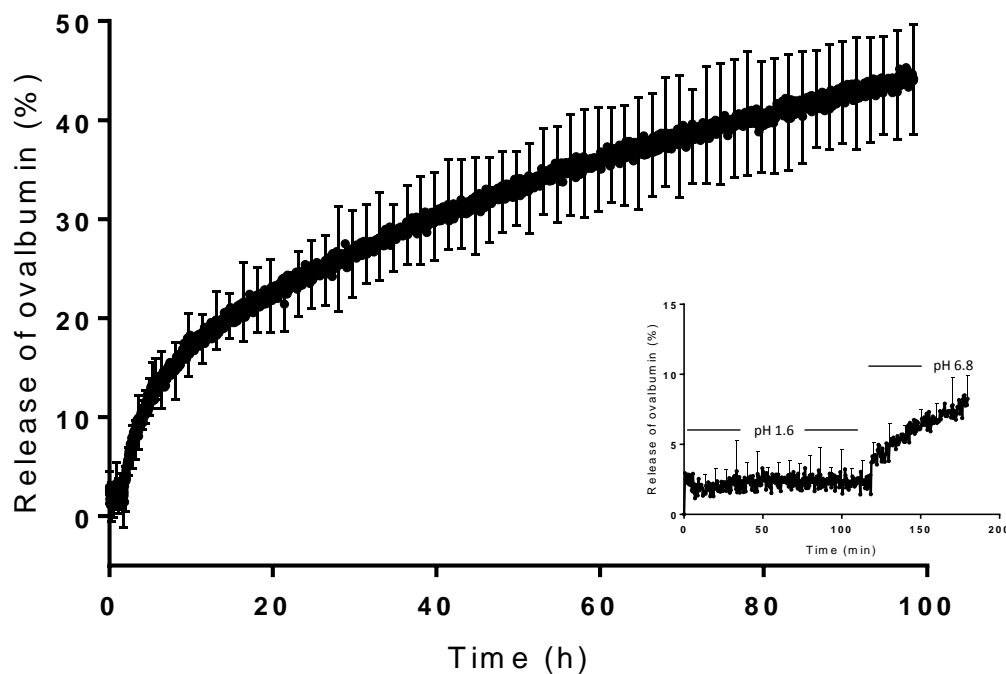
Fig. 6: SEM images of A) a cubosome-filled microcontainer, B) a filled microcontainers with a lid of Eudragit S100, and C) an empty microcontainer after release study in phosphate buffer pH 6.8.

Release of OVA loaded cubosomes from coated microcontainers

The coating on the cavity of the microcontainers can prevent the release until the intestine [33], and a large dose (approximately 2 μ g of powder) of the vaccine formulation can be loaded into the cavity of the microcontainers [27]. In the study, the cavity of the microcontainers was coated with the pH sensitive polymer Eudragit S100. The release of OVA from the cubosomes and microcontainers was first measured for 2 h in a pH value corresponding to the pH of the stomach (pH 1.6), and here, as expected, no release was observed due to the intact layer of the Eudragit lid (Fig. 7). After 2 h, the pH of the medium was changed to reflect that of the small intestine (pH 6.8). Fig. 7 shows that the release of OVA is occurring, and this indicate that the cubosomes are also released from the microcontainers as these are empty after the release studies (Fig. 6C). The release is appearing in a more controlled fashion than observed from the unconfined powder cubosomes (Fig. 4). The OVA release in pH 6.8 is 44.1 ± 5.6 % in relation to the amount of OVA in the particles. This is comparable to the release from the bulk powder being 47.9 % after 96 h (p-value: 0.4311).

In the literature, a rice-based oral vaccine has shown to be efficient as a delivery system as it can protect the antigen from enzymes in the stomach [7]. The microcontainers have the same feature and therefore, there is a promise for the microcontainers to work as an oral vaccine system as well. When delivering vaccines by the oral route, the delivery system should be able to present the vaccine formulation to the M cells followed by transport to the immune cells to create a response. It has been shown to be effective to

373 keep the vaccine formulation inside a particle for a significant period of time [10,12], securing a slow
 374 release. Therefore the slow release that the microcontainers and the cubosomes provide can be a great
 375 advantage when delivering vaccines.
 376



377
 378 Fig. 7: Release of OVA from the cubosomes, when the vaccine formulation was confined in microcontainers.
 379 The release of OVA is expressed as a % of the loaded OVA into the cubosomes. For the first 2 h the release
 380 was measured in pH 1.6 followed by pH of 6.8 for up to 98 h. The data is presented in triplicates as a
 381 mean \pm SD.
 382

383 Conclusion

384 Powder precursors of cubosomes loaded with OVA have been produced by spray drying, and it was
 385 concluded that the precursors contained cubic structure in bulk as well as when released from
 386 microcontainers. The microcontainers coated with an Eudragit S100 lid can serve as an oral vaccine delivery
 387 system protecting the cubosomes through the GI tract until release occurs in the small intestine. For these
 388 produced cubosomes to be completely developed as an oral vaccine system, an adjuvant needs to be
 389 added to the particles to obtain the optimal effect of this system and further investigations are therefore
 390 also needed for fully develop this oral vaccine delivery system.
 391

392 Acknowledgement

393 Assoc. Prof. Stephan Sylvest Keller is acknowledged for the fabrication of the SU-8 microcontainers, and the
 394 SAXS/WAXS beamline at the Australian Synchrotron is thanked as parts of these studies were performed
 395 there. Furthermore, the authors would like to thank the Danish Research Council for Technology and
 396 Production (FTP), Project DFF-4004-00120B for financial support, and in addition, the Danmarks

397 Grundforskningsfonds (project DNRF122) and Villum Fondens Center for Intelligent Drug Delivery and
398 Sensing Using Microcontainers and Nanomechanics (IDUN) is acknowledged.

399

Reference list

- 400 [1] Z. Zhao, K.W. Leong, Controlled delivery of antigens and adjuvants in vaccine development, *Journal*
401 *of Pharmaceutical Sciences*. 85 (1996) 1261–1270. doi:10.1021/js9602812.
- 402 [2] A.M. Stern, H. Markel, The History Of Vaccines And Immunization: Familiar Patterns, New
403 Challenges, *Health Affairs*. 24 (2005) 611–621. doi:10.1377/hlthaff.24.3.611.
- 404 [3] C. Czerkinsky, J. Holmgren, Vaccines against enteric infections for the developing world,
405 *Philosophical Transactions of the Royal Society B: Biological Sciences*. 370 (2015) 2–13.
406 doi:10.1098/rstb.2015.0142.
- 407 [4] A. Gebril, M. Alsaadi, R. Acevedo, A.B. Mullen, V.A. Ferro, Optimizing efficacy of mucosal vaccines.,
408 *Expert Review of Vaccines*. 11 (2012) 1139–55. doi:10.1586/erv.12.81.
- 409 [5] X.M. Chen, I. Elisia, D.D. Kitts, Defining conditions for the co-culture of Caco-2 and HT29-MTX cells
410 using Taguchi design, *Journal of Pharmacological and Toxicological Methods*. 61 (2010) 334–342.
411 doi:10.1016/j.vascn.2010.02.004.
- 412 [6] A. Azizi, A. Kumar, F. Diaz-Mitoma, J. Mestecky, Enhancing Oral Vaccine Potency by Targeting
413 Intestinal M Cells, *PLoS Pathogens*. 6 (2010) e1001147. doi:10.1371/journal.ppat.1001147.
- 414 [7] T. Nochi, H. Takagi, Y. Yuki, L. Yang, T. Masumura, M. Mejima, et al., Rice-based mucosal vaccine as a
415 global strategy for cold-chain- and needle-free vaccination., *Proceedings of the National Academy of*
416 *Sciences of the United States of America*. 104 (2007) 10986–10991. doi:10.1073/pnas.0703766104.
- 417 [8] M. Yu, M. Vajdy, Mucosal HIV transmission and vaccination strategies through oral compared with
418 vaginal and rectal routes., *Expert Opinion on Biological Therapy*. 10 (2010) 1181–95.
419 doi:10.1517/14712598.2010.496776.
- 420 [9] E. Sjögren, B. Abrahamsson, P. Augustijns, D. Becker, M.B. Bolger, M. Brewster, et al., In vivo
421 methods for drug absorption - comparative physiologies, model selection, correlations with in vitro
422 methods (IVIVC), and applications for formulation/API/excipient characterization including food
423 effects., 2014. doi:10.1016/j.ejps.2014.02.010.
- 424 [10] R.W. Ellis, Technologies for the design, discovery, formulation and administration of vaccines,
425 *Vaccine*. 19 (2001) 2681–2687. doi:10.1016/S0264-410X(00)00504-1.
- 426 [11] S.B. Rizwan, W.T. McBurney, K. Young, T. Hanley, B.J. Boyd, T. Rades, et al., Cubosomes containing
427 the adjuvants imiquimod and monophosphoryl lipid A stimulate robust cellular and humoral
428 immune responses, *Journal of Controlled Release*. 165 (2013) 16–21.
429 doi:10.1016/j.jconrel.2012.10.020.
- 430 [12] T. Storni, T.M. Kündig, G. Senti, P. Johansen, Immunity in response to particulate antigen-delivery
431 systems, *Advanced Drug Delivery Reviews*. 57 (2005) 333–355. doi:10.1016/j.addr.2004.09.008.
- 432 [13] A. Bolhassani, S. Safaiyan, S. Rafati, Improvement of different vaccine delivery systems for cancer
433 therapy., *Molecular Cancer*. 10 (2011) 3. doi:10.1186/1476-4598-10-3.
- 434 [14] Y. Fujikuyama, D. Tokuhara, K. Kataoka, R.S. Gilbert, J.R. McGhee, Y. Yuki, et al., Novel vaccine
435 development strategies for inducing mucosal immunity., *Expert Review of Vaccines*. 11 (2012) 367–
436 79. doi:10.1586/erv.11.196.
- 437 [15] N. Mishra, A.K. Goyal, S. Tiwari, R. Paliwal, S.R. Paliwal, B. Vaidya, et al., Recent advances in mucosal
438 delivery of vaccines: role of mucoadhesive/biodegradable polymeric carriers., *Expert Opinion on*
439 *Therapeutic Patents*. 20 (2010) 661–79. doi:10.1517/13543771003730425.
- 440 [16] A. Lancelot, T. Sierra, J.L. Serrano, Nanostructured liquid-crystalline particles for drug delivery.,
441 *Expert Opinion on Drug Delivery*. 11 (2014) 547–64. doi:10.1517/17425247.2014.884556.
- 442 [17] W. Leesajakul, M. Nakano, A. Taniguchi, T. Handa, Interaction of cubosomes with plasma
443 components resulting in the destabilization of cubosomes in plasma, *Colloids and Surfaces B:*
444 *Biointerfaces*. 34 (2004) 253–258. doi:10.1016/j.colsurfb.2004.01.010.
- 445 [18] S.B. Rizwan, D. Assmus, A. Boehnke, T. Hanley, B.J. Boyd, T. Rades, et al., Preparation of phytantriol
446 cubosomes by solvent precursor dilution for the delivery of protein vaccines, *European Journal of*
447 *Pharmaceutics and Biopharmaceutics*. 79 (2011) 15–22. doi:10.1016/j.ejpb.2010.12.034.

- 448 [19] S. Rizwan, T. Hanley, B. Boyd, T. Rades, S. Hook, Liquid Crystalline Systems of Phytantriol and
449 Glyceryl Monooleate Containing a Hydrophilic Protein: Characterisation, Swelling and Release
450 Kinetics, *Journal of Pharmaceutical Sciences*. 98 (2009) 4191–4204. doi:10.1002/jps.
- 451 [20] J. Kim, H. Kim, H. Chung, Y. Sohn, I. Kwon, S. Jeong, Drug formulations that form a dispersed cubic
452 phase when mixed with water, *Rel. Bioact. Mater.* 27 (2000) 1118–1119.
- 453 [21] P.T. Spicer, K.L. Hayden, M.L. Lynch, A. Ofori-Boateng, J.L. Burns, Novel process for producing cubic
454 liquid crystalline nanoparticles (cubosomes), *Langmuir*. 17 (2001) 5748–5756.
455 doi:10.1021/la010161w.
- 456 [22] P.T. Spicer, W.B. Small, M.L. Lynch, J.L. Burns, Dry powder precursors of cubic liquid crystalline
457 nanoparticles (cubosomes), *Journal of Nanoparticle Research*. 4 (2002) 297–311.
458 doi:10.1023/A:1021184216308.
- 459 [23] A.M. Avachat, S.S. Parpani, Formulation and development of bicontinuous nanostructured liquid
460 crystalline particles of efavirenz, *Colloids and Surfaces B: Biointerfaces*. 126 (2015) 87–97.
461 doi:10.1016/j.colsurfb.2014.12.014.
- 462 [24] M.A. Islam, J. Firdous, Y.J. Choi, C.H. Yun, C.S. Cho, Design and application of chitosan microspheres
463 as oral and nasal vaccine carriers: An updated review, *International Journal of Nanomedicine*. 7
464 (2012) 6077–6093. doi:10.2147/IJN.S38330.
- 465 [25] L.H. Nielsen, S.S. Keller, A. Boisen, A. Mullertz, T. Rades, A slow cooling rate of indomethacin melt
466 spatially confined in microcontainers increases the physical stability of the amorphous drug without
467 influencing its biorelevant dissolution behaviour, *Drug Deliv. and Transl. Res.* 4 (2014) 7.
- 468 [26] L.H. Nielsen, S.S. Keller, K.C. Gordon, A. Boisen, T. Rades, A. Mullertz, Spatial confinement can lead
469 to increased stability of amorphous indomethacin, *European Journal of Pharmaceutics and*
470 *Biopharmaceutics*. 81 (2012) 418–425. doi:10.1016/j.ejpb.2012.03.017.
- 471 [27] L.H. Nielsen, A. Melero, S.S. Keller, J. Jacobsen, T. Garrigues, T. Rades, et al., Polymeric
472 microcontainers improve oral bioavailability of furosemide, *International Journal of Pharmaceutics*.
473 504 (2016) 98–109. doi:10.1016/j.ijpharm.2016.03.050.
- 474 [28] L.M. Ensign, R. Cone, J. Hanes, Oral drug delivery with polymeric nanoparticles: The gastrointestinal
475 mucus barriers, *Advanced Drug Delivery Reviews*. 64 (2012) 557–570.
476 doi:10.1016/j.addr.2011.12.009.
- 477 [29] H.D. Chirra, L. Shao, N. Ciacchio, C.B. Fox, J.M. Wade, A. Ma, et al., Planar microdevices for enhanced
478 in vivo retention and oral bioavailability of poorly permeable drugs., *Advanced Healthcare Materials*.
479 3 (2014) 1648–54. doi:10.1002/adhm.201300676.
- 480 [30] C.L. Randall, T.G. Leong, N. Bassik, D.H. Gracias, 3D lithographically fabricated nanoliter containers
481 for drug delivery, *Advanced Drug Delivery Reviews*. 59 (2007) 1547–1561.
482 doi:10.1016/j.addr.2007.08.024.
- 483 [31] A. Ahmed, C. Bonner, T.A. Desai, Bioadhesive microdevices with multiple reservoirs: a new platform
484 for oral drug delivery, *Journal of Controlled Release*. 81 (2002) 291–306. doi:10.1016/s0168-
485 3659(02)00074-3.
- 486 [32] S.L. Tao, T.A. Desai, Aligned arrays of biodegradable poly(epsilon-caprolactone) nanowires and
487 nanofibers by template synthesis, *Nano Letters*. 7 (2007) 1463–1468. doi:10.1021/nl0700346.
- 488 [33] L.H. Nielsen, J. Nagstrup, S. Gordon, S.S. Keller, J. Østergaard, T. Rades, et al., pH-triggered drug
489 release from biodegradable microwells for oral drug delivery, *Biomedical Microdevices*. 17 (2015) 1–
490 7. doi:10.1007/s10544-015-9958-5.
- 491 [34] R.S. Petersen, S.S. Keller, A. Boisen, Hot punching of high-aspect-ratio 3D polymeric microstructures
492 for drug delivery., *Lab on a Chip*. 15 (2015) 2576–9. doi:10.1039/c5lc00372e.
- 493 [35] S. Keller, D. Haefliger, A. Boisen, Optimized plasma-deposited fluorocarbon coating for dry release
494 and passivation of thin SU-8 cantilevers, *Journal of Vacuum Science & Technology B:*
495 *Microelectronics and Nanometer Structures*. 25 (2007) 1903. doi:10.1116/1.2806960.
- 496 [36] S.S. Keller, F.G. Bosco, A. Boisen, Ferromagnetic shadow mask for spray coating of polymer patterns,
497 *Microelectronic Engineering*. 110 (2013) 427–431. doi:10.1016/j.mee.2013.03.029.

- 498 [37] N.M. Kirby, S.T. Mudie, A.M. Hawley, D.J. Cookson, H.D.T. Mertens, N. Cowieson, et al., A low-
 499 background-intensity focusing small-angle X-ray scattering undulator beamline, *Journal of Applied*
 500 *Crystallography*. 46 (2013) 1670–1680. doi:10.1107/S002188981302774X.
- 501 [38] A.A. Ambike, K.R. Mahadik, A. Paradkar, Stability study of amorphous valdecoxib, *International*
 502 *Journal of Pharmaceutics*. 282 (2004) 151–162. doi:10.1016/j.ijpharm.2004.06.009.
- 503 [39] C.J. Drummond, C. Fong, Surfactant self-assembly objects as novel drug delivery vehicles, *Current*
 504 *Opinion in Colloid and Interface Science*. 4 (1999) 449–456. doi:10.1016/S1359-0294(00)00020-0.
- 505 [40] M.F. Bachmann, G.T. Jennings, Vaccine delivery: a matter of size, geometry, kinetics and molecular
 506 patterns., *Nature Reviews. Immunology*. 10 (2010) 787–96. doi:10.1038/nri2868.
- 507 [41] M. Hori, H. Onishi, Y. Machida, Evaluation of Eudragit-coated chitosan microparticles as an oral
 508 immune delivery system, *International Journal of Pharmaceutics*. 297 (2005) 223–234.
 509 doi:10.1016/j.ijpharm.2005.04.008.
- 510 [42] J. Myschik, F. Eberhardt, T. Rades, S. Hook, Immunostimulatory biodegradable implants containing
 511 the adjuvant Quil-A - Part I: Physicochemical characterisation, *Journal of Drug Targeting*. 16 (2008)
 512 213–223. doi:10.1080/10611860701848860.
- 513 [43] H. Aomori, T. Ishiguro, K. Kuwata, T. Kaneko, K. Ogino, Study on thermal and structural behavior of
 514 monoacylglycerol-water systems. II. The phase behavior of monooleoylglycerol-water systems.,
 515 *Journal of Japan Oil Chemists' Society*. 44 (1995) 1004–1011. doi:10.1017/CBO9781107415324.004.
- 516 [44] H. Qiu, M. Ca, The phase diagram of the monoolein / water system : metastability and equilibrium
 517 aspects, *Biomaterials*. 21 (2000) 223–234.
- 518